Kinetics of the low-temperature selective catalytic reduction of NO with NH_3 over activated carbon fiber composite-supported iron oxides

Gregorio Marbán * and Antonio B. Fuertes

Instituto Nacional del Carbón (CSIC), Apartado 73, 33080-Oviedo, Spain

Received 29 April 2002

A kinetic analysis in a variety of conditions (gas composition and temperature) has been conducted on catalysts of iron oxides supported on activated carbon fiber composites (ACFC). Additionally, experiments of temperature-programmed desorption (TPD) of NO were conducted on the catalysts in order to reveal mechanistic features of the low-temperature SCR reaction. In the light of current SCR literature and previous work, a qualitative picture of the catalytic behavior of low-temperature SCR catalysts is offered. Apparently, the strength of adsorption of NO during the low-temperature SCR reaction is responsible for the governing reaction mechanism. Thus, highly stable nitrates formed on the surface provoke catalyst deactivation and reaction through an ER mechanism, with NO reacting from the gas phase, whereas the absence of these nitrates permits reaction of less stable nitrites from the catalyst surface, following an LH-type mechanism. This is the case for the ACFC-supported iron oxide catalyst analyzed in this work.

KEY WORDS: selective catalytic reduction; activated carbon fibers; composites; kinetics; iron oxides.

1. Introduction

The selective catalytic reduction (SCR) of NO with NH_3 ($4NO + 4NH_3 + O_2 \rightarrow 4N_2 + 6H_2O$) is a well-established de-nitrification procedure that can be applied to remove NO efficiently from the flue gas of combustion units. In recent years, there has appeared a growing interest on developing catalysts which are active for SCR at low temperature (<200 °C), thus permitting one to operate in the tail end of the combustion plant, where the gases are almost free of particulates and other catalyst deteriorating agents (SO_2, arsenic, etc.). However, there is an unparalleled number of research works on kinetics of low-temperature SCR catalysts, probably because this is a complex task, due in part to the occurrence of strong adsorption phenomena. Therefore, these kinetic studies have been undertaken by a small number of researchers. Among them, two Dutch groups [1,2] have been very active in the analysis of catalysts consisting of manganese oxides supported on γ-alumina. A first approach of Kijlstra *et al.*, as indicated in [2], was to fit the reaction-rate data obtained in an integral reactor to the exponential equation

$$r_c = k p_{NO}^{a} p_{NH_3}^{b} p_{O_2}^{c} = \mathrm{mol_{NO}\ g_{cat}^{-1}\ s^{-1}} \qquad (1)$$

in which the values of a, b and c were 0.79, −0.04 and 0.51. Then, after some transient and infrared studies [3,4] that led them to postulate that NO is reduced in two parallel reaction steps (Eley–Rideal (ER) and Langmuir–Hinshelwood (LH), though the major part of N_2 is produced by the ER step), these authors derived a set of kinetic equations with the purpose of corroborating their postulated mechanism [2]. Similarly, Kapteijn *et al.* [1] performed a series of kinetic studies on an Mn-based catalyst (Mn_2O_3-WO_3/γ-Al_2O_3) and found slightly different reaction orders, especially in the NO partial pressure, that fitted the exponential equation (1) in the temperature range 110–150 °C ($a = 0.39$–0.44; $b = 0$; $c = 0.33$–0.47). Based on previous literature, these authors postulated the following LH-type reaction scheme:

$$O_2 + 2\bigstar \leftrightarrows 2\bigstar - O \qquad (a)$$

$$NO + \bigstar - O \leftrightarrows \bigstar - NO_2 \qquad (b)$$

$$NH_3 + \square \leftrightarrows \square - NH_3 \qquad (c)$$

$$\square - NH_3 + \bigstar - O \rightarrow \square - NH_2 + \bigstar - OH \qquad (d)$$

$$\square - NH_2 + \bigstar - NO_2 \rightarrow N_2 + H_2O + \bigstar - O \qquad (e)$$

$$2\bigstar - OH \leftrightarrows H_2O + \bigstar - O + \bigstar. \qquad (f)$$

Contrary to the postulates of Kijlstra *et al.*, which were posterior in time, this mechanism neglects the ER step and considers that NO reacts from an adsorbed state. Fitting criteria proved the convenience of assuming a Freundlich-type NO adsorption for reaction (b). The consideration of two different adsorption sites for NO (★) and NH_3 (□), which are close to each other, came from the infrared results published by other authors [5]. On the basis of the steady-state assumption, further assumptions, as irreversibility of steps (d) and (e) and strong adsorption of NH_3 (no empty □-sites), led to

* To whom correspondence should be addressed.
E-mail: greca@incar.csic.es

1011-372X/02/1100-0013/0

the following kinetic expression, firstly reported in ref. [6]:

$$r_c = \frac{k_1 p_{NO}^n p_{O_2}^{0.5}}{1 + K_2 p_{O_2}^{0.5}(1 + K_3 p_{NO}^n) + K_4 p_{O_2}^{0.25} p_{H_2O}^{0.5}} \quad (2)$$

where n ($0 < n < 1$) is the coefficient of the Freundlich isotherm ($[\bigstar - NO_2] = K_b \times p_{NO}^n \times [\bigstar - O]$), $k_1 = k_e K_a^{0.5} K_b C_{\bigstar} s$, $K_2 = K_a^{0.5}$, $K_3 = K_b$ and $K_4 = K_a^{0.25} K_f^{-0.5}$. In k_1, s represents the average number of □-sites neighboring the ★-sites [6]. This pioneering work yielded, however, some uncertainty in the values of the constants, those in the denominator of equation (2) being zero in most of the cases (thus reverting to the exponential equation). In a later work, Kapteijn *et al.* [7] arrived at the same conclusions as Kijlstra *et al.* [4] for an Mn_2O_3/γ-Al_2O_3 catalyst; this is a combined ER/LH reaction.

A close view of the whole set of works dealing with low-temperature SCR systems reveals the important role of adsorbed NO species during reaction. The works commented on in the above paragraphs refer to the role of NO as reactant, which can be in part in an adsorbed state (LH mechanism). During the SCR reaction some deactivation by NO chemisorption can also occur. This has been reported for CuO/Al_2O_3 catalysts [8] and manganese oxides supported on γ-alumina [3], and on activated carbon fibers [9,10] and nickel oxides supported on activated carbon fibers [10]. Kijlstra *et al.* [3] indicate that formation of bidentate and bridged nitrates on the active centers competes with NH_3 adsorption during the SCR reaction, thus lowering the activity of an MnO_x/Al_2O_3 catalyst. Previously, Centi and Perathoner [8] had explored the self-deactivation of CuO/Al_2O_3 catalysts by formation of bidentate nitrates on the catalyst surface. We also found an inverse relation between the amount of NO chemisorbed in an SCR environment and the achieved NO conversion for a given catalyst of manganese oxides supported on a Nomex-based monolith [9].

Although the main purpose of this work is to obtain reliable kinetic parameters for a highly active ACF-supported iron-based low-temperature SCR catalyst, whose preparation was optimized in a previous work [10], it also pursued a deeper understanding on the reaction mechanism that permits us to draw a qualitative picture of the low-temperature SCR reaction as a function of the type of catalyst (active phase) used.

2. Experimental

2.1. Catalyst preparation

The fabrication of Nomex-based support is thoroughly described in ref. [11]. Briefly, the Nomex rejects were carbonized in N_2 at 850 °C, milled by conventional blade-mills and sieved to obtain a sieved fraction of size 0.1–0.4 mm. This fraction was dry-mixed with powdered phenolic resin (Novolak) in a mass ratio 3:1. The mixture was then cured in a cylindrical mould for 75 min at a temperature of 180 °C. The cured composite was carbonized in N_2 at 700 °C.

For the preparation of the Fe-based catalyst that was used for the kinetic studies, the carbonized support was activated at 40 wt% (weight loss) in a quartz reactor at 700 °C with a stream of water (steam, ~25 vol%) in N_2. The activated monolith was oxidized with HNO_3 (40 vol%) at 90 °C for 1 h. A concentrated solution of iron(III) nitrate was prepared and a given volume of the solution (with a value similar to that of the support pore volume) was used to impregnate the preconditioned support with a known amount of metal. Afterwards, the catalyst was dried in a forced convection oven at 60 °C for 2 h and then at 120 °C for 2 h. Finally, the catalyst was heat-treated in N_2 at 400 °C for 1 h. The iron content of the catalyst was 6.3 wt%. This catalyst will be referred to as Fe-40-PVI (table 1). In a previous work of the authors [10], this catalyst was found to be the most active catalyst (in catalyst weight basis) among a group of ACFC-supported catalysts of iron, manganese, vanadium, chromium and nickel oxides.

Other Fe-based catalysts were prepared in order to gain insight into the NO adsorption modes which might be relevant in the low-temperature SCR reaction mechanism. These catalysts were prepared by impregnation of ACFCs with different activation degrees, with aqueous solutions of iron nitrates. Table 1 offers the

Table 1
Catalysts prepared in this work.

Reference	Metal	Support burnoff (wt%)	Support oxidation	Impregnation method	% Metal (wt%)
Fe-40-PVI [a]	Fe	40	HNO_3 90 °C 1 h	PVI [b]	6.3
Fe-20-PVI	Fe	20	HNO_3 90 °C 1 h	PVI	1.4
Fe-50-PVI	Fe	50	HNO_3 90 °C 1 h	PVI	6.9
Fe-50-NaEA	Fe	50	HNO_3 90 °C 2 h	Na-EA	2.9
Fe-50-EA	Fe	50	HNO_3 90 °C 2 h	EA	3.9

[a] Standard catalyst used for kinetic experiments.
[b] PVI: Pore volume impregnation; EA: Equilibrium adsorption; Na-EA: Equilibrium adsorption with a previous step of NaOH exchange.

acronyms and the most relevant features of all the catalysts used in this work. For a complete description of the catalyst preparation methods, refer to ref. [9,10,23].

2.2. Characterization

Temperature-programmed desorption (TPD) of NO from given samples of ACFC-supported catalysts (~0.9 cm height and ~0.6 cm diameter) was carried out in a vertical quartz reactor (0.65 cm i.d.) connected to an Omnistar model mass spectrometer. Before the TPD, the sample was treated at 125 °C with a 150 mL min^{-1} stream of NO (700 ppm$_v$) and O_2 (3 vol%) in He for 1 h. Then the gas was changed into He stream for 1 h at the same temperature in order to release all physically adsorbed NO. In the TPD, an He flow rate of 150 mL min^{-1} was used with a temperature increase rate of 5 °C min^{-1} from 125 to 400 °C. The NO released during the TPD stage was used to calculate the total amount of NO chemisorbed in the presence of oxygen. The results are expressed as molar ratios of adsorbed NO to metal weight (NO/Met, $mol_{NO}\,mol_{met}^{-1}$).

In principle it would seem more appropriate to perform the TPD experiments with NH_3, which is known to react from an adsorbed state during the SCR reaction, and therefore could be used to characterize the active surface. However, previous experiments showed that NH_3 chemisorption by the support itself (without metal) contributed to ~35% of the total NH_3 chemisorbed by the catalyst at temperatures below 175 °C, and thus a totally unbiased analysis of the TPD curves was not possible. A pre-adsorption temperature of 125 °C was chosen in order to minimize the effect of NO adsorption by the carbonaceous support, which was found to be negligible in the presence of O_2 at the referred temperature.

2.3. Catalytic activity tests—kinetic analysis

The catalytic activity tests were conducted under isothermal conditions. In a standard test, a cylindrical catalyst (~0.9 cm height and ~0.6 cm diameter) was fixed by means of a teflon strip to the inner wall of a vertical quartz reactor (0.65 cm i.d.), thus sealing the space between the catalyst and the tube wall. The reactor was electrically heated in a Carbolite furnace. Before each experiment, the sample was dried in He at 200 °C for around 20 min. The total gas flow was 300 mL min^{-1}. The inlet gas was a mixture of 700 ppm$_v$ NO, 800 ppm$_v$ NH_3, 3 vol% O_2 and He to balance. The NO/NO_2 concentration of the inlet ($C^0_{NO_x}$) and outlet (C_{NO_x}) gases was analyzed by means of a chemiluminiscence analyzer (Rosemount Analytical; Model 951A). Before entering the gas analysis system, the gases were bubbled through an aqueous solution of phosphoric acid (3–20 wt%) in order to remove the NH_3. The degree of NO_x disappearance, X, was evaluated from the change in NO_x concentration between the inlet and outlet gases at steady-state conditions [$X = (C^0_{NO_x} - C_{NO_x})/C^0_{NO_x}$]. With this configuration and for the experimental conditions used (catalyst weight ≈60 mg; GHSV ≈ 70 000 h^{-1}; $T = 150$ °C) the maximum observed reaction rates fell into the range associated with kinetic control, with no diffusion restrictions (internal, external or axial) according to the standard criteria [12–17]. The apparent kinetic constant based on supported metal mass, k_m, was calculated as [9,10,23]:

$$k_m = \frac{1}{p^0_{NO_x}}\left(\frac{F^0_{NO}}{w_m}\right)\ln\frac{1}{1-X} = mol_{NO}\,g_{met}^{-1}\,s^{-1}\,Pa^{-1} \quad (3)$$

where $p^0_{NO_x}$ is the inlet partial pressure of NO_x and F^0_{NO}/w_m is the actual inlet NO molar flow per metal weight.

For the kinetic analysis, catalytic activity tests under differential conditions were performed. The catalyst was crushed and the resulting powder was mixed with ~0.9 g of inert SiC particles (74 μm) in a catalyst/SiC mass ratio in the range 0.011–0.015, and introduced in the vertical reactor. The effects on the differential reaction rate of temperature and NO, NH_3 and O_2 partial pressures were analyzed in the ranges 125–200 °C, 20–130 Pa, 80–165 Pa and 0–7000 Pa, respectively, at a total pressure of 1.01×10^5 Pa, for the selected iron-based catalyst (Fe-40-PVI). During the experiments the catalyst weight was selected so that the NO conversion degree was never over 0.1 (differential reactor). The reaction rate was then calculated as

$$r_c = \frac{F^0_{NO}X}{w_c} = mol_{NO}\,g_{cat}^{-1}\,s^{-1} \quad (4)$$

where w_c is the mass of catalyst. The maximum observed reaction rates fell into the range associated with kinetic control, with no diffusion restrictions (internal, external or axial) according to the standard criteria [12–17]. The experimental values of the reaction rate were fitted to empirical kinetic and mechanistic functions of temperature, NO, NH_3 and O_2 partial pressures, as described in the corresponding section.

3. Results and discussion

3.1. Low-temperature SCR reaction mechanism

In a former work [10], the role of NO adsorption on the low-temperature SCR mechanism was discussed. This was done by performing TPD-NO experiments, following the same procedure as that indicated in the Experimental section, with ACFC-supported Fe-, Mn-, V-, Cr- and Ni-oxide catalysts. For analyzing the TPD curves, a deconvolution method thoroughly described in the literature [18,19,22] was followed. The

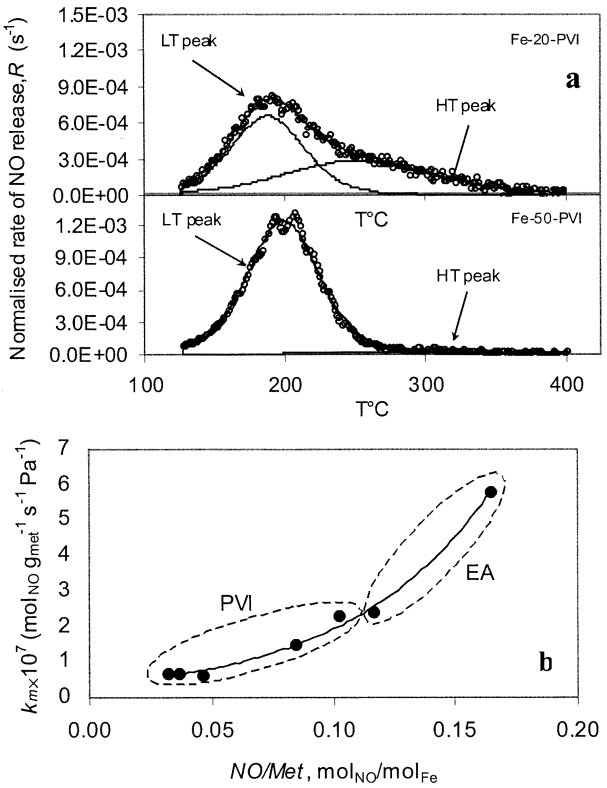

Figure 1. TPD experiments of Fe-catalysts. (a) Normalized rate of NO release *versus* temperature for Fe-based catalysts obtained by PVI; (b) Relation between total NO released in metal weight basis during the TPD of NO and catalytic activity on metal mass basis at 150 °C (k_m).

main observations achieved are summarized here:

- The curves of NO desorption rate *versus* temperature obtained with the ACFC-supported catalysts are formed by two desorption peaks: a low-temperature peak (LT peak) centered at ~200 °C and a high-temperature peak (HT peak) centered at ~250 °C. Examples of these curves are given in figure 1(a).
- The Mn- and Ni-based catalysts display a high (HT peak)/(LT peak) area ratio (~5). On the other hand, highly dispersed Fe-, Cr- and V-based catalysts only present an LT peak. For these catalysts the apparent kinetic constant based on supported metal mass, k_m, was directly related to the total amount of NO desorbed per metal weight (LT peak area).

These results can be compared to those obtained by Kijlstra *et al.* [4] in experiments of TPD of NO from manganese oxides supported on γ-alumina, which were previously submitted to $NO + O_2$ adsorption at 50 °C. These authors found two unconnected TPD peaks (heating rate = 5 °C min^{-1}), centered at 137 °C (peak range: 50–230 °C) and 327 °C (peak range: 230–425 °C), respectively. Since the TPD experiments performed for the ACFC-supported catalysts were commenced at 125 °C, the LT peak might correspond to the far end of the first peak found by Kijlstra *et al.*, which they attributed to desorption of linearly coordinated and monodentate nitrites and bridged nitrites. The relation between k_m and LT peak area corroborates the conclusion of Kijlstra *et al.* [3], according to whom NO species desorbed in this peak can probably react with contiguously adsorbed NH_3 in SCR conditions, and therefore do not diminish, but contribute to, the catalyst activity. On the other hand, the HT peak takes place at a much lower temperature than the second peak observed by Kijlstra *et al.* (~250 *versus* 327 °C). This fact suggests a lower stability of the NO complexes formed on the manganese/nickel oxides supported on the carbonaceous surface. According to the values of thermal stabilities for different NO complexes given by these authors, the HT peak displayed by the ACFC-supported catalysts might well correspond to desorption of bridged nitrates or bidentate nitrates "type I". These species are rather stable in the low-temperature SCR environment [3,8] and could occupy a fraction of active centers, with the corresponding decrease of the catalytic activity for the Mn- [9] and Ni-based catalysts [10] induced by increased NO chemisorption.

Thus, there seem to be two different adsorption modes of NO, which in the TPD of NO are represented by a low-temperature desorption peak (LT peak) and a high-temperature desorption peak (HT peak). As already commented, according to Kijlstra *et al.* [4] adsorbed NO corresponding to the LT peak (monodentate and bridged nitrites) can react with contiguously adsorbed NH_3 during the SCR reaction. It can be speculated that thermally stable NO on the catalyst surface (HT peak) would need higher temperatures than those prevailing in the low-temperature SCR regime to react with NH_3, and therefore adsorbed NH_3 which is surrounded only (isolated) by thermally stable NO complexes (HT peak) would only be able to react with NO from the gas phase. Thus, for a high HT peak/LT peak area ratio NO would react preferentially from the gas phase (ER mechanism) whereas for a low ratio (predominance of LT peak) surface reaction (LH or Freundlich) would occur to a larger extent. Additionally, as already stated by Kijlstra *et al.* [4] NO desorbed in the HT peak contributes to catalyst deactivation by blocking active centers for SCR reaction. These authors also stated that the rate of formation of stable nitrates is lower in the presence of NH_3. This is consistent with a mechanism of formation of nitrates from previously formed nitrites [4]. Thus, when nitrites are formed they can either react with NH_3 to N_2 or be oxidized to stable nitrates. Deactivation would occur when a site for adsorption of NH_3 is completely surrounded by stable nitrates. It must also occur that the intrinsic reactivity between NO and NH_3 is higher in the LH mechanism than in the ER mechanism; otherwise, the ER mechanism would always be the dominant path. From above, a catalyst stable in the long-term should display a TPD-NO pattern with a high LT peak and no HT peak. The values of k_m at 150 °C of the catalysts

presenting only the LT peak (highly dispersed Cr-, V- and Fe-based catalysts) correlate well with this trend [10], *i.e.*, the higher the LT peak area, the more active the catalyst. The obvious question is whether catalysts of similar nature can show different (HT peak/LT peak) area ratios or not. In fact this is quite so for the catalysts prepared by Kijlstra *et al.* and Kapteijn *et al.*, as inferred from the experiments of TPD-NO reported by these groups [4,5]. Additionally, in this work we encountered strong differences in the TPD patterns for Fe-based catalysts obtained under different preparation conditions (table 1). A clear example is indicated by the TPD-NO experiments shown in figure 1(a), where it can be seen that an iron-based catalyst prepared by PVI of a low-activated support (20 wt% act.) produces a significant amount of NO in the HT peak, whereas for the Fe-catalyst prepared from a highly activated support the HT peak is almost absent. This also suggests that the formation of stable nitrates is related to the dispersion degree of the active phase; the more dispersed the catalyst the lower the amount of stable nitrates formed, which would also explain the loss of activity of ACFC-supported Ni-based catalysts for increasing Ni loadings [10]. The kinetic analysis described below corresponds to an Fe catalyst prepared on the highly activated (40 wt%) support (Fe-40-PVI). In principle, from the above considerations, the absence of an HT peak in the TPD profile for this catalyst suggests an LH reaction path for the SCR reaction. This will be analyzed in the following: *A priori* for all the Fe-based catalysts prepared in this work, both by PVI and EA (or NaEA), as indicated in table 1, a clear relation between the amount of desorbed NO during the TPD experiments and the catalytic activity at 150 °C in metal mass basis (k_m) is observed (figure 1(b)), which strongly suggests reaction of NO from an adsorbed state.

3.2. Kinetic analysis of ACFC-supported Fe-based catalyst

A common characteristic of previous kinetic studies is to consider no reaction in the absence of oxygen. Here, SCR experiments in the absence of oxygen were performed for different temperatures and NO partial pressures, with the results shown in figure 2. As observed, the reaction rate is about two orders lower in the absence of oxygen, though its relative ratio cannot be considered negligible (*e.g.*, the achieved differential conversion at 150 °C was 0.013 in the absence of O_2 and 0.084 for $p_{O_2} = 3040$ Pa). A first approach to the reaction kinetics for this catalyst is to consider the common exponential equation, both in the absence and in the presence of oxygen:

$$r'_c = k' p_{NO}^a = \mathrm{mol_{NO}\ g_{cat}^{-1}\ s^{-1}} \qquad p_{O_2} = 0 \qquad (5)$$

$$r_c = k p_{NO}^a p_{NH_3}^b p_{O_2}^c = \mathrm{mol_{NO}\ g_{cat}^{-1}\ s^{-1}} \qquad p_{O_2} > 0. \quad (1a)$$

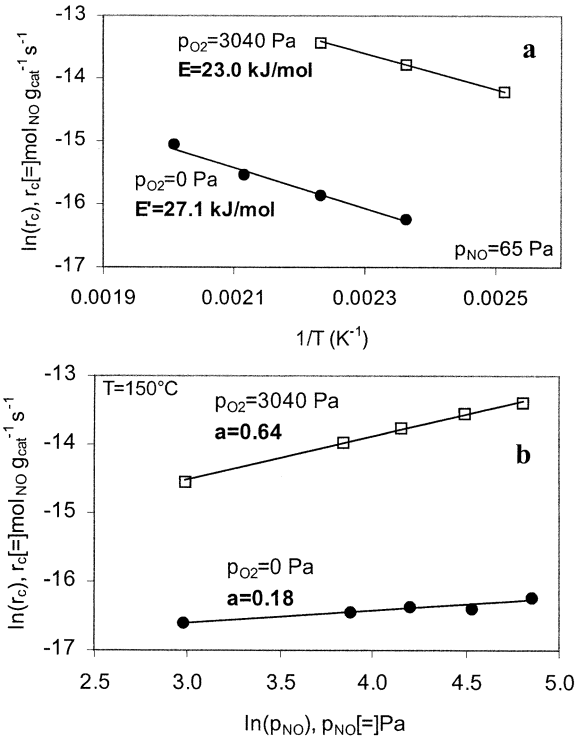

Figure 2. Comparison of differential reaction rates in the absence and presence of O_2 at different temperatures and NO partial pressures. The indicated activation energies and reaction orders (a) were obtained by data fittings to the exponential equations (1) and (5).

For all the analyzed temperatures and gas compositions, selectivity values were in every case over 0.9, so that N_2O formation can be disregarded in the following discussion. Table 2 shows the reaction orders and Arrhenius parameters obtained in the absence [equation (5)] and in the presence of oxygen [equation (1)]. Figure 3 shows the experimental values (symbols) of the differential reaction rate for three different temperatures (125, 150 and 175 °C) obtained at varying NO (figure 3(a)), NH_3 (figure 3(b)) and O_2 (figure 3(c)) partial pressures. The dashed curves represent the best fittings to equation (1), with the Arrhenius parameters and average reaction orders indicated in table 2. As expected, the reaction order in the NH_3 partial pressure is close to zero, though at the lowest temperature (125 °C) it is slightly negative. According to Singoredjo *et al.* [1,6] the reaction order with respect to ammonia on Mn_2O_3-WO_3/γ-Al_2O_3 is slightly negative at 110 °C. These authors propose that NO adsorbs on a different site than ammonia, but ammonia can also compete with NO on its adsorption sites, thus inhibiting the reaction when NO reacts from an adsorbed state. Another feature of this exponential analysis is that the reaction order in the NO partial pressure in the absence of oxygen is lower than that in the presence of oxygen. The lack of other results prevents us from inferring a conclusive reaction mechanism in the absence of oxygen. Unpublished experiments recently undertaken by our group on carbon-supported

Table 2
Kinetic results for the ACFC-supported iron-based catalyst (Fe-40-PVI).

$r_c = k p_{NO}^a p_{NH_3}^b p_{O_2}^c = \text{mol}_{NO}\,g_{cat}^{-1}\,s^{-1}$						$r_c' = k' p_{NO}^a = \text{mol}_{NO}\,g_{cat}^{-1}\,s^{-1}$			
T (°C)	a	b	c	Exponential equation		a	Exponential equation		
125	0.54	−0.18	0.39	$p_{O_2} > 0$, $k = k_0 \exp(-E/RT)$		–	$p_{O_2} = 0$, $k' = k_0' \exp(-E'/RT)$		
150	0.64	−0.05	0.40	–	–	0.18	–	–	
175	0.65	0.01	0.42	k_0 ($\text{mol}_{NO}\,g_{cat}^{-1}\,s^{-1}\,Pa^{-(a+b+c)}$)	E (kJ mol^{-1})	–	k_0' ($\text{mol}_{NO}\,g_{cat}^{-1}\,s^{-1}\,Pa^{-a}$)	E' (kJ mol^{-1})	
<avg.>	0.61	−0.08	0.40	3.01×10^{-6}	23.0	0.18	8.94×10^{-5}	27.1	

LH-type (Freundlich) reaction equation

$$r_c = r_c' + \frac{k_1 p_{NO}^n p_{O_2}^{0.5}}{1 + K_2 p_{O_2}^{0.5}(1 + K_3 p_{NO}^n)} = \text{mol}_{NO}\,g_{cat}^{-1}\,s^{-1}$$

$k_1 = k_{1,0} \exp(-E_1/RT)$

$K_2 = K_{2,0} \exp(-E_2/RT)$; $K_3 = K_{3,0} \exp(-E_3/RT)$

$k_{1,0}$ ($\text{mol}_{NO}\,g_{cat}^{-1}\,s^{-1}\,Pa^{-(0.5+n)}$)	$K_{2,0}$ ($Pa^{-0.5}$)	$K_{3,0}$ (Pa^{-n})	n	E_1 (kJ mol^{-1})	E_2 (kJ mol^{-1})	E_3 (kJ mol^{-1})
1.29×10^{-5}	2.21×10^{1}	1.32×10^{-4}	0.89	33.3	26.3	−18.1

Mn-based catalysts suggest a mechanism similar to that depicted by equations (a)–(f), though in the absence of O_2 oxidation of the active centers [reaction (a)] is carried out by NO itself, which is therefore reduced to N_2. This mechanism is also described in the review by Busca *et al.* [20]. Nevertheless, the kinetic parameters obtained for reaction in the absence of oxygen, r_c' (table 2), can be used to detach this contribution from the overall reaction rate in the presence of oxygen. With this assumption, and returning to the LH mechanism emphasized above, the following kinetic expression is obtained:

$$r_c = r_c' + \frac{k_1 p_{NO}^n p_{O_2}^{0.5}}{1 + K_2 p_{O_2}^{0.5}(1 + K_3 p_{NO}^n)} = \text{mol}_{NO}\,g_{cat}^{-1}\,s^{-1}. \quad (6)$$

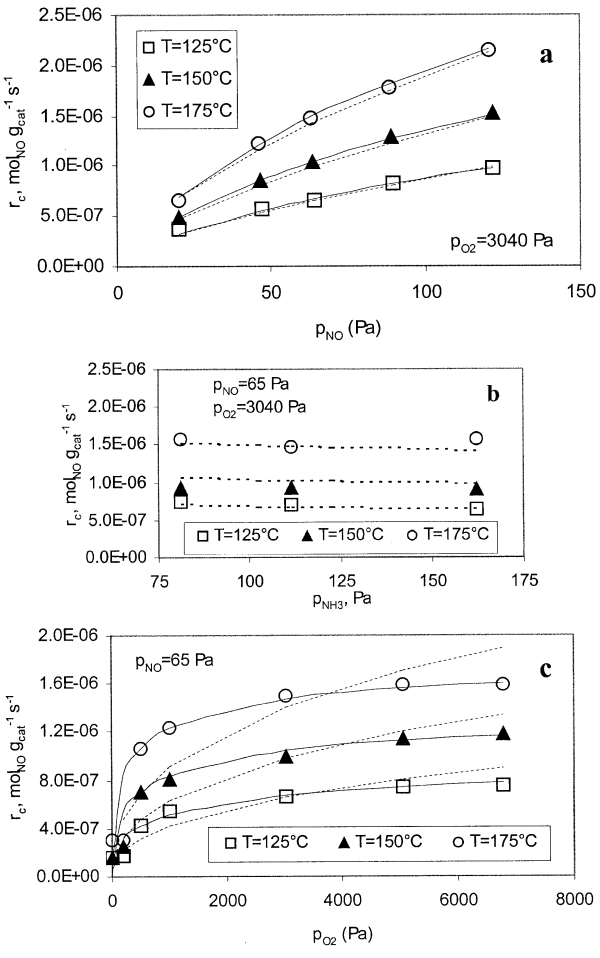

Figure 3. Experimental values of the differential reaction rate (symbols) and corresponding fittings to the exponential equation (dashed curves) and the LH-type (Freundlich) reaction equation (continuous curves) for different temperatures and (a) NO, (b) NH_3 and (c) O_2 partial pressures.

This expression is similar to that used by Kapteijn *et al.* [equation (2)], which was derived by considering the set of reactions (a)–(f). Only the following differences are introduced: (i) equation (6) considers the parallel occurrence of reaction without the participation of oxygen, r_c'; and (ii) in equation (6) the effect of reaction (f) is neglected ($p_{H_2O} \approx 0$ under the imposed differential conditions). The continuous curves in figure 3 represent the best fittings to equation (6), with the different Arrhenius parameters indicated in table 2. As observed, there is a remarkable agreement between experimental and model results, which supports the proposed LH-type mechanism. The value obtained for n (0.89) indicates that the adsorption of NO is almost ideal (LH). The activation energies shown in table 2 are composite solutions of the reaction enthalpies of reactions (a) and (b) and activation energy of reaction (e): $E_1 = E_e + \frac{1}{2}\Delta H_a + \Delta H_b$; $E_2 = \frac{1}{2}\Delta H_a$; $E_3 = \Delta H_b$. With these relationships, the following true kinetic parameters are obtained: $\Delta H_a = 52.7\,\text{kJ mol}^{-1}$ (oxidation of the active centers), $\Delta H_b = -18.1\,\text{kJ mol}^{-1}$ (NO adsorption) and $E_e = 25.1\,\text{kJ mol}^{-1}$ (SCR reaction). The negative value for ΔH_b is a clear indication of an exothermic adsorption process. The value of the activation energy for reaction (e) is similar to that obtained by Kapteijn *et al.* [1] for their manganese-based catalysts. From a review carried out by Marangozis [21] on a number of kinetic studies of high-temperature SCR catalysts, an average intrinsic activation energy for the SCR reaction of $56.4 \pm 17.6\,\text{kJ mol}^{-1}$ (24 catalysts) can be derived. Considering that NO reacts from the gas phase for the high-temperature systems, both values of activation energy (25.1 and 56.4) may well express the difference between the LH and the ER reactions.

4. Conclusions

A microkinetic analysis was performed on an ACFC-supported Fe-based catalyst, obtained by PVI of an activated (40 wt%) carbon fiber support. The differential reaction rates obtained under a number of gas compositions and temperatures could be successfully fitted to a kinetic rate expression derived from an LH-type mechanism. In general, it seems that for any catalyst the strength of adsorption of NO during the low-temperature SCR reaction is responsible for the governing reaction mechanism. Thus, highly stable nitrates formed on the surface provoke catalyst deactivation and reaction through an ER mechanism, with NO reacting from the gas phase, whereas the absence of these nitrates permits reaction of less stable nitrites from the catalyst surface, following an LH-type mechanism, as is the case of the Fe-based catalyst analyzed in this work.

Acknowledgments

The financial support of the European Coal and Steel Community (Project 7220-PR042) is acknowledged. We also thank the Spanish Ministry of Science and Technology (MCyT) for financial support (Acción Especial MAT 2000–0314-CE). Finally, we thank DuPont Ibérica S.A. for the supply of Nomex rejects.

References

[1] F. Kapteijn, L. Singoredjo, N.J.J. Dekker and J.A. Moulijn, Ind. Eng. Chem. Res. 32 (1993) 445–452.
[2] W.S. Kijlstra, D.S. Brands, E.K. Poels and A. Bliek, Catal. Today 50 (1999) 133–140.
[3] W.S. Kijlstra, D.S. Brands, H.I. Smit, E.K. Poels and A. Bliek, J. Catal. 171 (1997) 219–230.
[4] W.S. Kijlstra, D.S. Brands, E.K. Poels and A. Bliek, J. Catal. 171 (1997) 208–218.
[5] G. Ramis, G. Busca, F. Bregani and P. Forzatti, Appl. Catal. 64 (1990) 243–259.
[6] L. Singoredjo, PhD Thesis, University of Amsterdam, 1992.
[7] F. Kapteijn, L. Singoredjo, M. van Driel, A. Andreïni, J.A. Moulijn, G. Ramis and G. Busca, J. Catal. 150 (1994) 105–116.
[8] G. Centi and S. Perathoner, J. Catal. 152 (1995) 93–102.
[9] G. Marbán and A.B. Fuertes, Appl. Catal. B: Environ. 34(1) (2001) 55–71.
[10] G. Marbán, R. Antuña and A.B. Fuertes, *Low-temperature SCR of NO_x with NH_3 over Activated Carbon Fiber Composite-supported Metal Oxides*, Appl. Catal. B: Environ. submitted.
[11] G. Marbán, A.B. Fuertes and D.M. Nevskaia, Carbon 38 (2000) 2167–2170.
[12] R.B. Bird, W.E. Stewart and E.N. Lightfoot, *Transport Phenomena*, sec. 17–28 (John Wiley & Sons, NY, 1982).
[13] J.A. Moulijn, A. Tarfaoui and F. Kapteijn, Catalysis Today 11 (1991) 1–12.
[14] O. Levenspiel, *The Chemical Reactor Omnibook*, Chaps. 22–23 (OSU Book Stores, Oregon, USA, 1996).
[15] L.K. Doraiswamy and M.M. Sharma, *Heterogeneous reactions: Analysis, examples and reactor design*. Vol. I: *Gas–solid and solid–solid reactions*, Chap. 3 (John Wiley & Sons, NY, 1984).
[16] R.B. Bird, W.E. Stewart and E.N. Lightfoot, *Transport Phenomena*, sec. 1–23, 21–48 (John Wiley & Sons, NY, 1982).
[17] L.K. Doraiswamy and M.M. Sharma, *Heterogeneous reactions: Analysis, examples and reactor design*. Vol. I: *Gas–solid and solid–solid reactions*, Chap. 6 (John Wiley & Sons, NY, 1984).
[18] M.J.G. Alonso, D. Álvarez, A.G. Borrego, R. Menéndez and G. Marbán, Energy & Fuels 15 (2001) 413–428.
[19] G. Marbán and A. Cuesta, Energy & Fuels 15 (2001) 764–766.
[20] G. Busca, L. Lietti, G. Ramis and F. Berti, Appl. Catal. B: Environ. 18 (1998) 1–36.
[21] J. Marangozis, Ind. Eng. Chem. Res. 31 (1992) 987–994.
[22] G. de la Puente, G. Marbán, E. Fuente and J.J. Pis, J. Anal. Appl. Pyrol. 44 (1998) 205–218.
[23] G. Marbán and A.B. Fuertes, Appl. Catal. B: Environ. 34(1) (2001) 43–53.